Supporting Information

Synthesis, crystal structures and luminescent properties of tetranuclear Zn molecular clusters with aroylhydrazone ligand

Bei-bei Tang,[a] Heng Ma, [a] Guan-zheng Li, [a] Yue-bing Wang,[a] Gulinazi Anwar,[a] Rufei Shi,[b] Hui Li [a]*

[a] *Key Laboratory of Cluster Science of Ministry of Education, School of Chemistry, Beijing Institute of Technology, Beijing 100081, P. R. China.*

E-mail: lihui@bit.edu.cn; Fax: +86-10-68912667

[b] *Department of Chemistry, Loras College, Dubuque, Iowa 52001, USA*

Contents

Section 1 Synthesis of the Ligand H_3L, 1 and 2

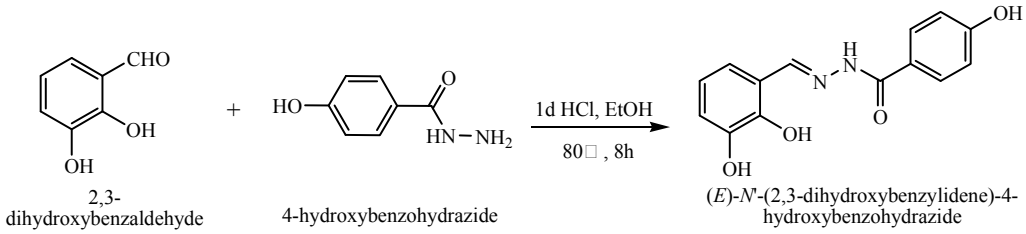

Scheme S1 Synthetic route of the ligand H_3L.

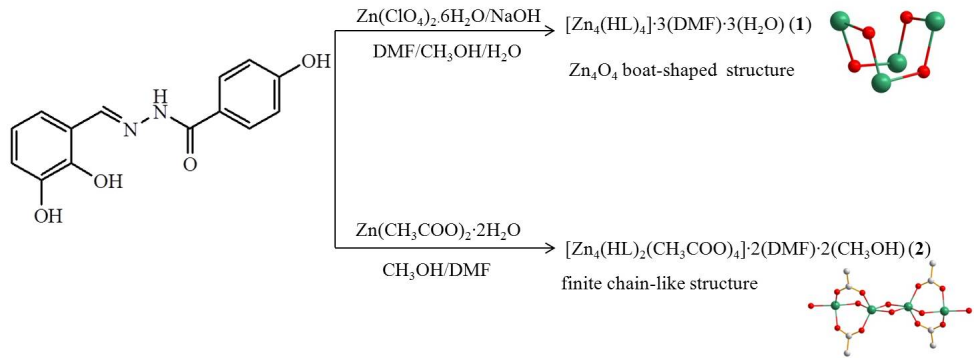

Scheme S2 The reaction representations of the molecular clusters **1** and **2**.

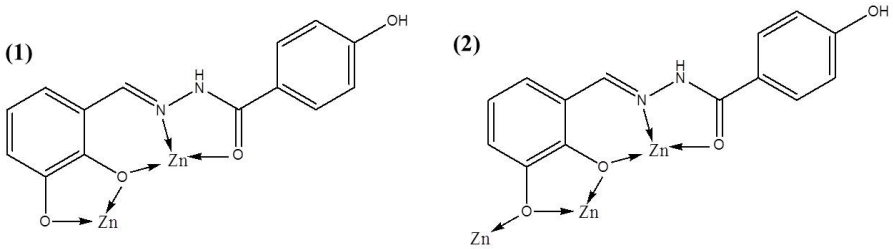

Scheme S3 (a) The η^1: η^2: η^1: η^1:μ_2 chelating/bridging mode of HL^{2-} ligand in **1** and (b) the η^2: η^2: η^1: η^1:μ_3 chelating/bridging mode of HL^{2-} ligand in **2**

Section 2 Selected Bond Distances (Angles) and Distances (Angles) of Hydrogen Bonds of 1 and 2

Table S1 Selected Bond Distances (Å) and Angles (deg) for **1**[a] and **2**[b]

		1	
Zn(1)-O(2)	1.988(5)	Zn(2)-O(7)	2.068(5)
Zn(1)-O(1)	2.010(4)	Zn(2)-N(2)	2.093(6)
Zn(1)-O(1)#1	2.028(4)	O(5)-Zn(2)-O(7)	143.44(19)
Zn(1)-N(1)	2.083(4)	O(5)-Zn(2)-N(2)	84.45(19)
Zn(1)-O(3)	2.092(4)	O(5)#3-Zn(2)-O(7)	101.54(18)
O(1)-Zn(1)#2	2.028(4)	O(2)-Zn(1)-O(1)	110.79(19)

Zn(2)-O(6)	1.973(5)	O(1)-Zn(1)-O(3)	149.67(17)
Zn(2)-O(5)#3	2.013(4)	O(1)#1-Zn(1)-N(1)	163.63(19)
Zn(2)-O(5)	2.020(4)		
		2	
Zn(1)-O(6)	1.9874(19)	Zn(2)-O(4)#1	2.0681(18)
Zn(1)-O(8)	1.9886(17)	Zn(2)-Zn(2)#1	3.1574(12)
Zn(1)-O(3)	1.9903(17)	O(6)-Zn(1)-O(8)	111.88(7)
Zn(1)-O(2)	2.0833(17)	O(3)-Zn(1)-O(2)	160.70(6)
Zn(1)-N(1)	2.087(2)	O(8)-Zn(1)-N(1)	131.73(8)
Zn(2)-O(7)	1.9742(18)	O(7)-Zn(2)-O(4)	102.27(7)
Zn(2)-O(4)	1.9909(16)	O(7)-Zn(2)-O(5)	113.14(8)
Zn(2)-O(3)	2.0211(16)	O(4)-Zn(2)-O(3)	155.42(7)

[a]Symmetry transformations used to generate equivalent atoms: #1 y,-x+1,-z+1, #2 -y+1, x,-z+1, #3 y-1,-x+1,-z.

[b]Symmetry transformations used to generate equivalent atoms: #1 -x,-y+1,-z+1.

Table S2 Distances (Å) and Angles (°) of Hydrogen Bonds for **1** and **2**

D—H···A	d(H···A)	d(D···A)	∠D—H···A
		1	
O(4)–H(4a)···O(6)	1.788	2.606	175.77
O(8)–H(8a)···O(2)	1.709	2.528	177.83
N(4)–H(6a)···O(10)	1.994	2.797	154.94
N(7)–H(21a)···O(11)	2.039	2.811	149.01
		2	
C(23c)–H(23L)···O(6)	2.452	3.391	168.0
N(2)–H(2)···O(10a)	2.041	2.860	158.9

Section 3 Structural Information for 1 and 2.

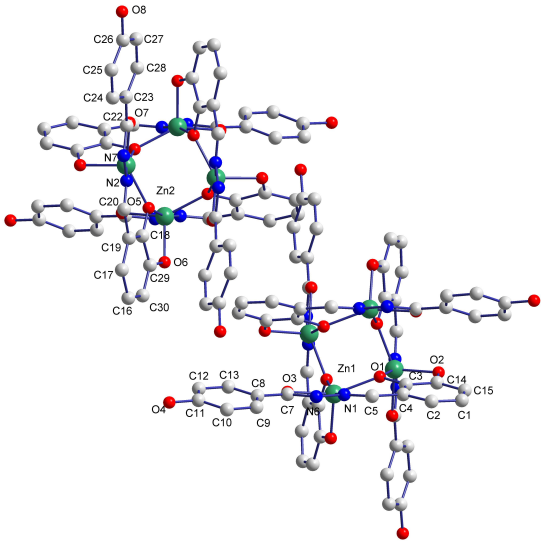

Fig. S1 The two crystallographically independent tetranuclear molecular cluster $[Zn(L)]_4$

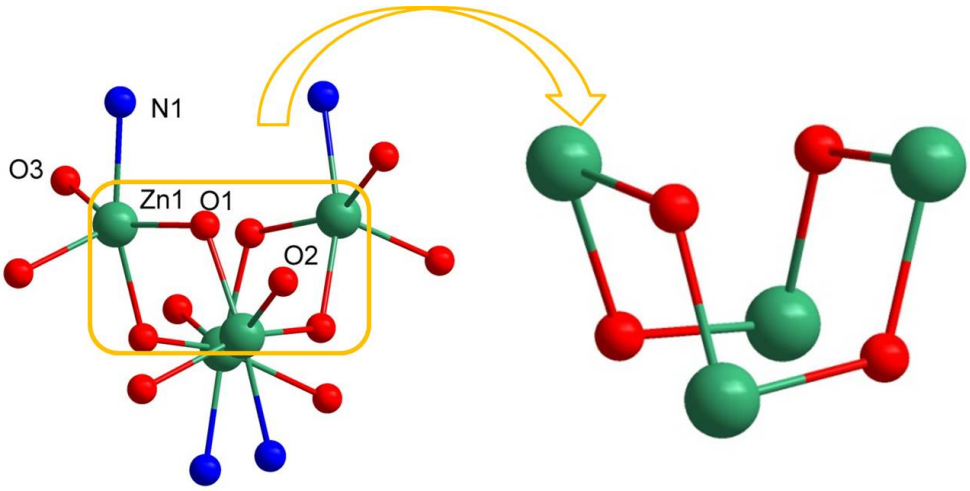

Fig. S2 The boat-shaped conformation of Zn_4O_4 core in **1**. Color scheme: Zn, green; O, red

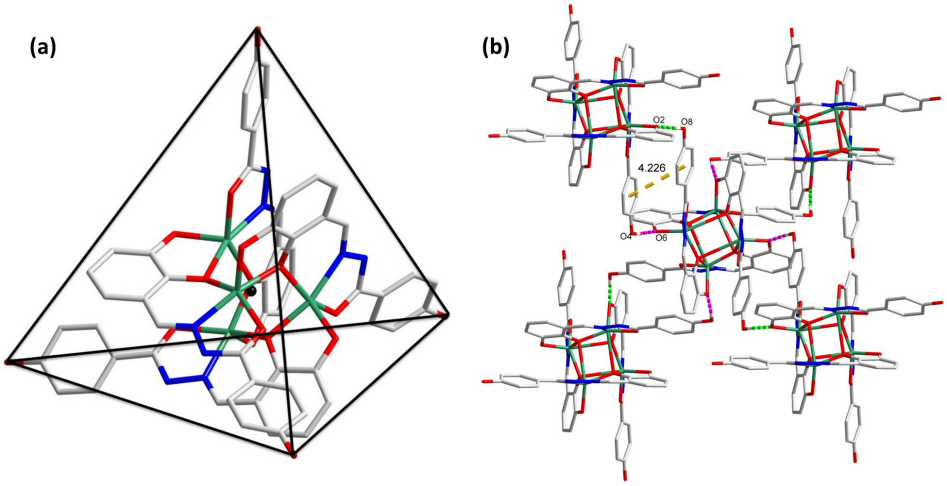

Fig. S3 (a) Molecular structure of $[Zn_4(HL)_4]$ unit in **1**. The black ball is the center of four Zn atoms and the black solid lines show the distorted tetrahedral geometry of the $[Zn_4(HL)_4]$ unit. (b)The H-bonding and π-π stacking interaction linked the molecule of **1** with four neighbor molecules (O8 – H8···O2: green dashed line; O4 – H8···O6: pink dashed line; π-π stacking interaction: yellow dashed line)

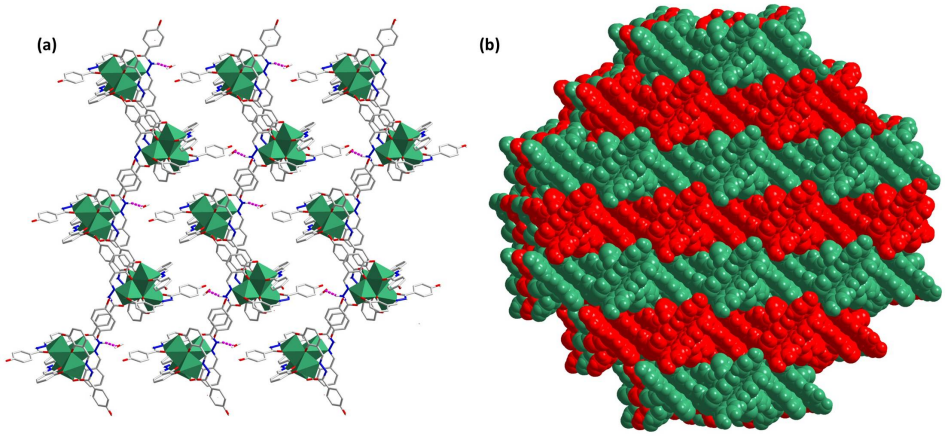

Fig. S4 (a) Hydrogen bonds with N – H···O type (pink dashed line) in 3D two-fold interpenetrated structure.(b)The 3D space-filling packing picture of **1**, showing independent 3D networks in red and green.

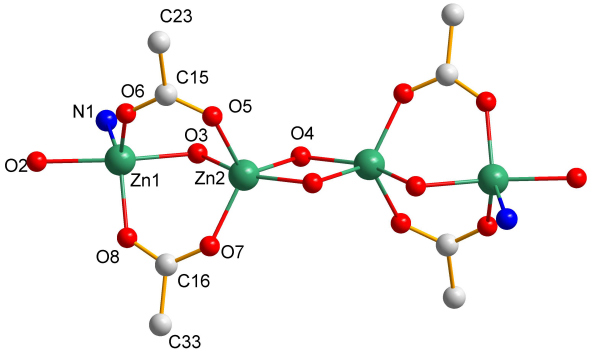

Fig. S5 the finite 1D chain core in **2**.

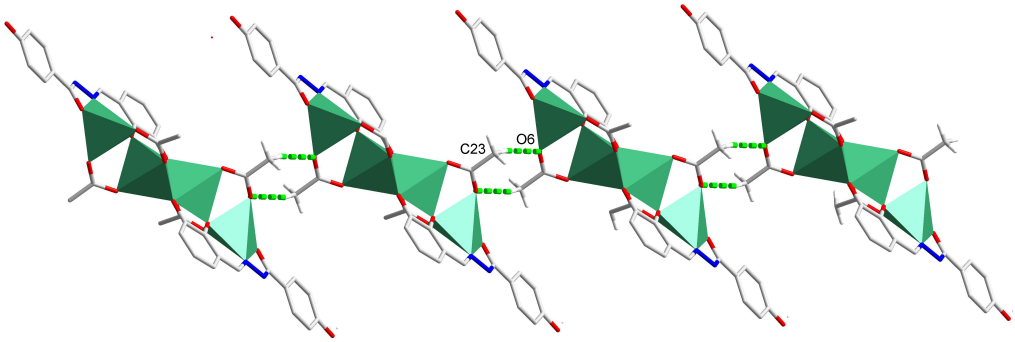

Fig. S6 The polyhedral representations of the 1D chain structure in **2** by H-bonding .

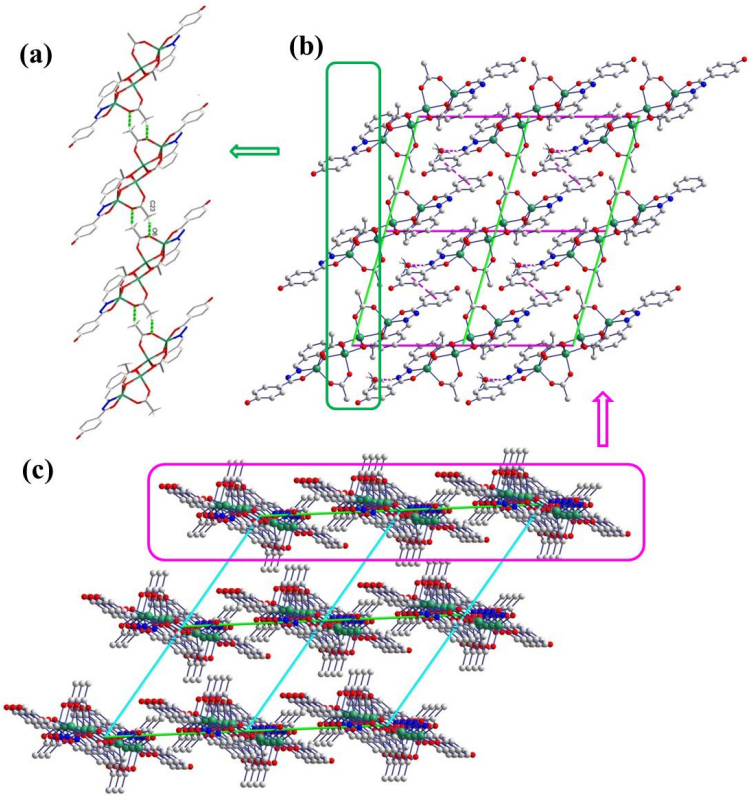

Fig. S7 (a) The 1D chain structure of molecular cluster **2** by H-bonding C–H···O (green line); (b) The 2D layer structure of **2** by H-bonding O–H···O and N–H···O view down from *b* axis (pink line); (c) The 3D packing picture of **2** by Van de Waals interaction viewed down from *a* axis (blue line).

Section 4 IR spectrum, TGA Curves and PXRD patterns for 1 and 2.

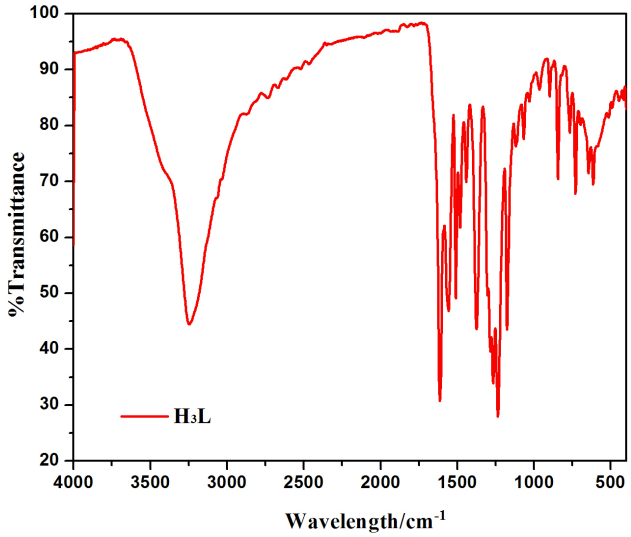

(a)

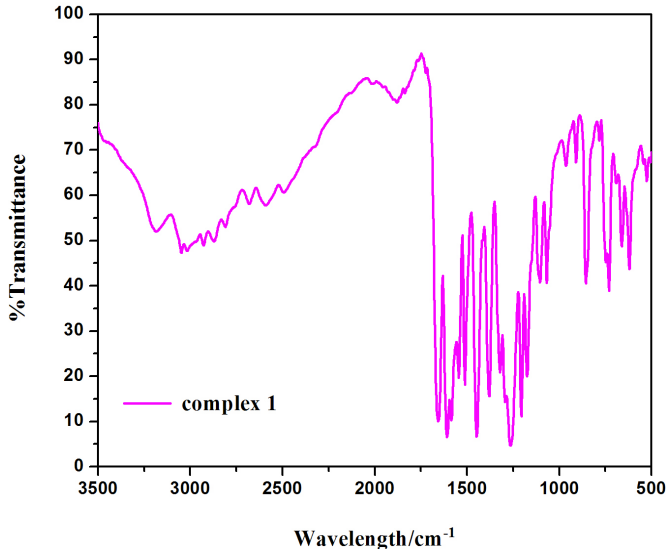

(b)

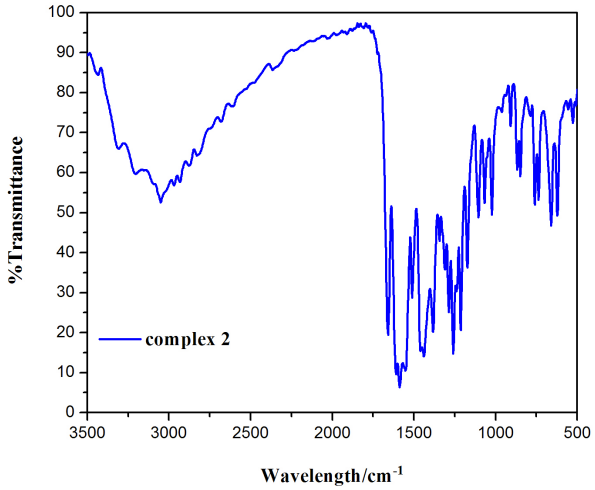

(c)

Fig. S8 IR spectra for (a) **H_3L**, (b) **1** and (c) **2**

The simulated and experimental XRPD patterns of the two molecular clusters are shown in Fig. S9. All the peaks displayed in the measured patterns match up with those in the simulated patterns generated from single-crystal diffraction data. Their peak positions are in good agreement with each other, indicating the phase purity of the products.

The thermogravimetric analytical (TGA) studies were performed from 35°C to 800 °C at a ramp rate of 10 °C/min in a flowing 150 mL/min nitrogen atmosphere (Fig. S10). The TGA curve of **1** displays three distinct stages of weight losses. The first stages is from 35 to 76 °C corresponds to the loss of three lattice water molecules. The observed weight loss of 3.18% is in agreement with the calculated value of 3.36%. The second is from 200 to 270 °C corresponds to the loss of three DMF molecules of 13.71% (calculated 13.65%). The complex remains 3D diamondoid framework up to around 350 °C. This result supported the conclusion that **1** is stable that can be compared with 3D coordination-bonded polymer. For **2**, the weight loss (5.01%) before 106 °C corresponds to the release of two solvent methanol molecules (calculated 5.13%). A weight loss of 11.21% between 130 and 215 °C is in accordance with the release of two DMF molecules (calculated 11.71%). The molecular cluster **2** will be decomposed around 300 °C. Compared with **1**, the molecular cluster **2** is with less thermal stability.

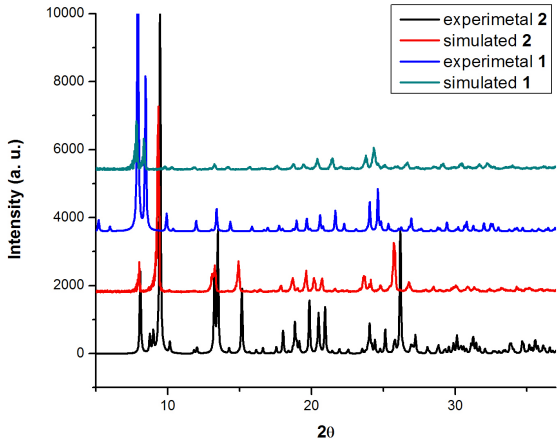

Fig. S9 Simulated and experimental XRPD spectra of molecular cluster **1** and **2**.

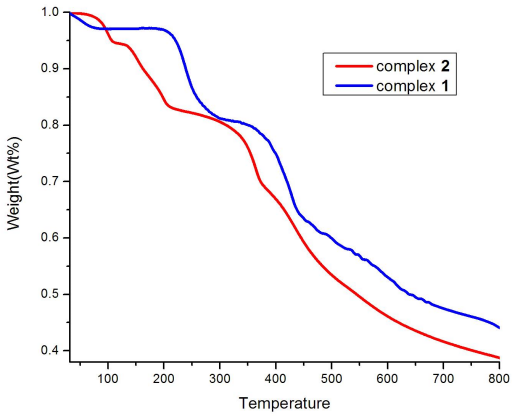

Fig. S10 Thermogravimetric profiles in the temperature range 35-800°C for molecular cluster **1** and **2**.

Section 5 ^{1}H NMR, ^{13}CNMR and MS Studies

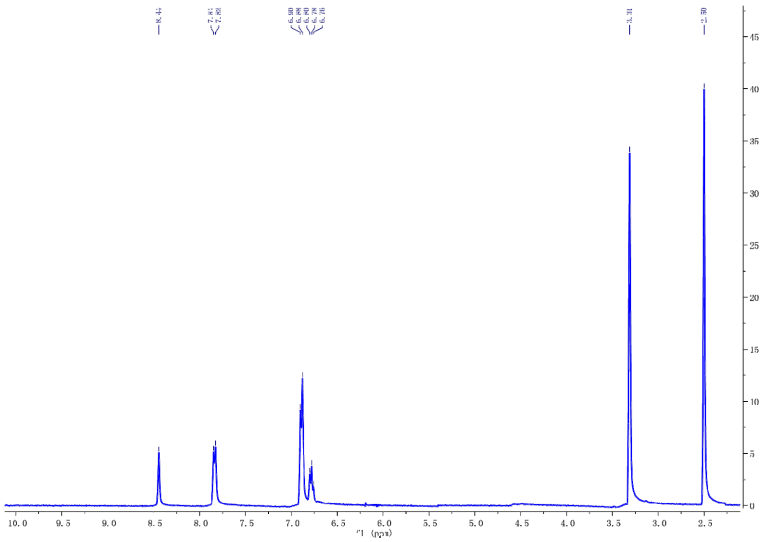

Fig. S11 ^{1}H NMR spectra of the ligand **H_3L** in d^{6}-DMSO solution.

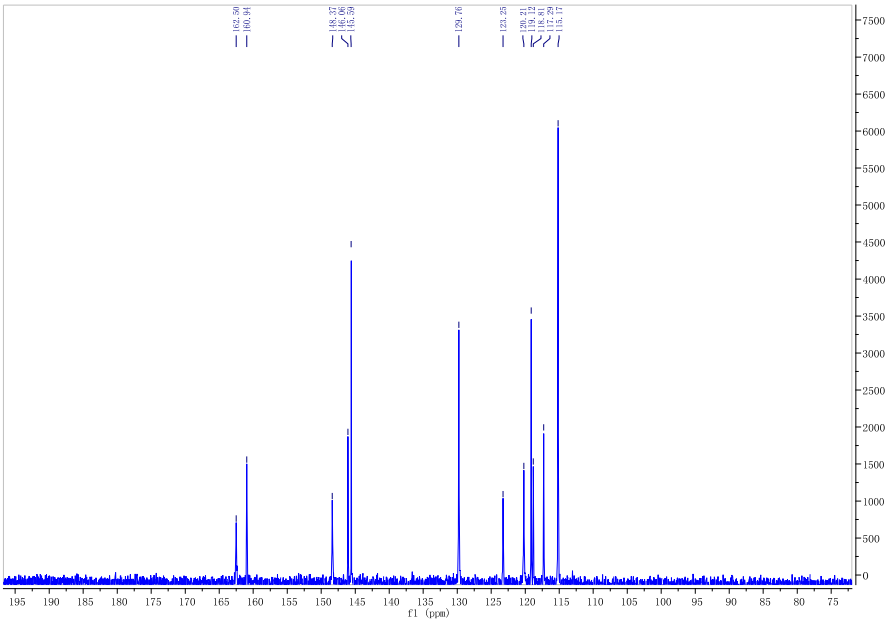

Fig. S12 ^{13}CNMR spectra of the ligand **H_3L** in d^{6}-DMSO solution.

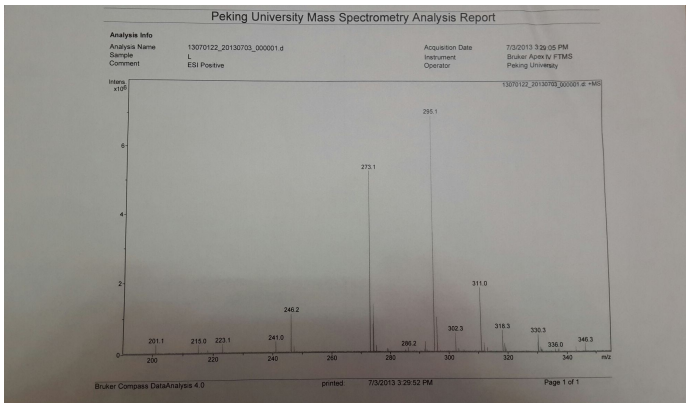

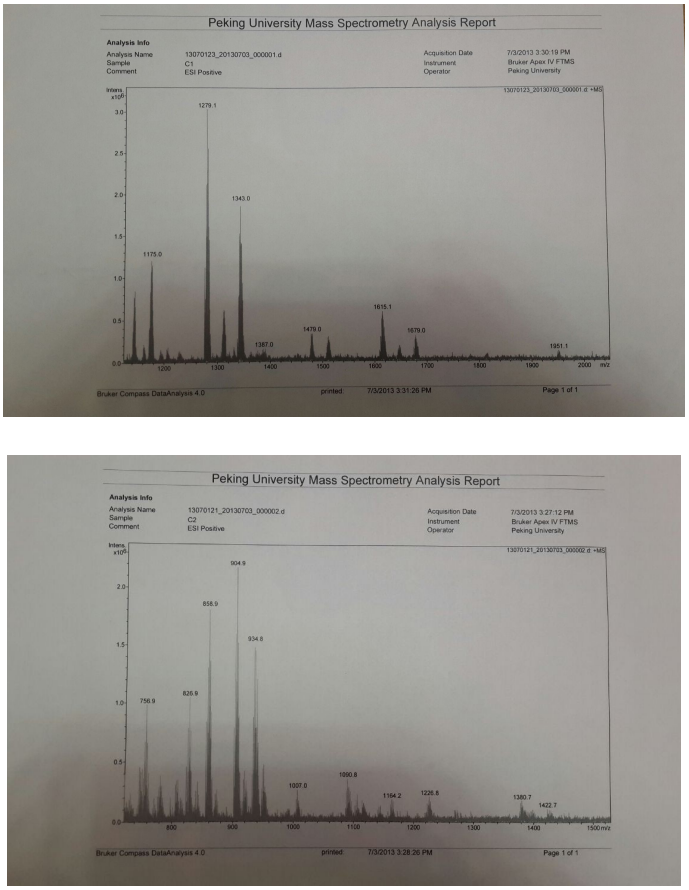

Fig. S13 ESI-MS of the ligand **H_3L,** complex **1** and **2** in d^6-DMSO solution.

Section 6 UV-Vis absorption and emission spectra in solution

According to the ESI-MS spectrum shown (Fig. S13) in the complexes, some decomposition occurred. In **1**, the peak at 1615.1 corresponds to **1** and the peak at 1343.0 corresponds to loss of one ligand. In **2**, some decomposition occurred, too. Even though, **1** and **2** were still keeping their complexes forms with slight structure alterations (according to mass spectra data). The electronic absorption spectra of the ligand **H_3L**, **1** and **2** in solution are shown in Fig. S14a. The ligand presents two important transitions with absorption bands at 258 and 305 nm corresponding to carbonyl C=O bond and imine C=N bond.[1] In the molecular cluster **1** and **2,** these bands exhibited a red shift and appear at ~280, 330nm for **1** and ~280, 338nm for **2**. These changes could be attributed to the interaction between the ligand moiety and zinc. The binding of **H_3L** to Zn^{2+} can form a six-membered chelate ring with the Schiff base C=N and Ar–O-, which enlarges the conjugated system, and reduces the energy difference between n and π* orbital. [1]

The photoluminescence behaviors of the ligand **H_3L**, molecular cluster **1** and **2** were studied(Fig. S14b). The maximum fluorescent emission for **H_3L**, **1** and **2** were observed at 483,

496 and 513 nm respectively, which is based on the intra-ligand energy transition (IL). Compared with the emission spectra of the ligand, the red shift for coordination complexes may be due to that the coordination of Zn(II) ions enhances the ligand's ability to accept electrons and decreases the electron transition energy. As a result, the HOMO–LUMO energy gap of the complexes decreases.[2]

The photoluminescence properties of molecular cluster **1** and **2** in various solvents are studied with its crystalline samples dissolved in solvents such as H_2O, DMSO, DMF, CH_3CN, CH_3OH, C_2H_5OH, i-PrOH, acetone, CH_2Cl_2 and THF (Fig. S14c and S14d). The polarities of these solvents are in the following order: H_2O > DMSO > CH_3OH > DMF> CH_3CN > acetone > C_2H_5OH ~ i-PrOH > THF > CH_2Cl_2. The emission phenomena for **1** and **2** differ in different solvents and range from 439 to 505nm and 439 to 544nm, respectively. In **1**, the emissions from long to short wavelength are in the following order: H_2O > CH_3OH~ C_2H_5OH ~ i-PrOH > DMSO >DMF> acetone > THF > CH_3CN > CH_2Cl_2, and the emission wavelength corresponds to the solvent polarity. As mentioned above, in solvents with higher polarity like H_2O, DMSO, DMF, CH_3OH, molecular cluster **1** emits a longer wavelength comparing with that in THF, CH_2Cl_2, and acetone. It is worth noting that ethanol and i-PrOH is polar proton solvents and is known as a strong H-bonding Donor (HBD). Therefore, the emission wavelengths of the molecular cluster **1** were also red-shifted in ethanol and i-PrOH. Molecular cluster **1** in CH_3CN emits a shorter wavelength compared with that in the other higher polarity solvents. This is due to that CH_3CN is regarded as uncoordinating solvents. In **2**, the emissions from long to short wavelength are in the following order: THF> CH_3CN > CH_3OH~ C_2H_5OH ~ i-PrOH> H_2O> DMSO >DMF> acetone > CH_2Cl_2 and the emission wavelength depends both on the solvent polarity and H-bonding Donor (HBD) effect. Its emission red shifts in CH_3CN, CH_3OH, C_2H_5OH, i-PrOH, H_2O, DMSO and DMF, comparing with CH_2Cl_2 and acetone. Meanwhile, in CH_2Cl_2, CH_3CN and THF, the emissions are not only found around such positions at 439, 533 and 544 nm, respectively, but also at wavelength of 550, 447 and 450 nm. On the basis of the above analysis, the solvent effects on photophysical properties of **1** and **2** are examined and both **1** and **2** exhibit a wide range of luminescence in the different organic solvents.

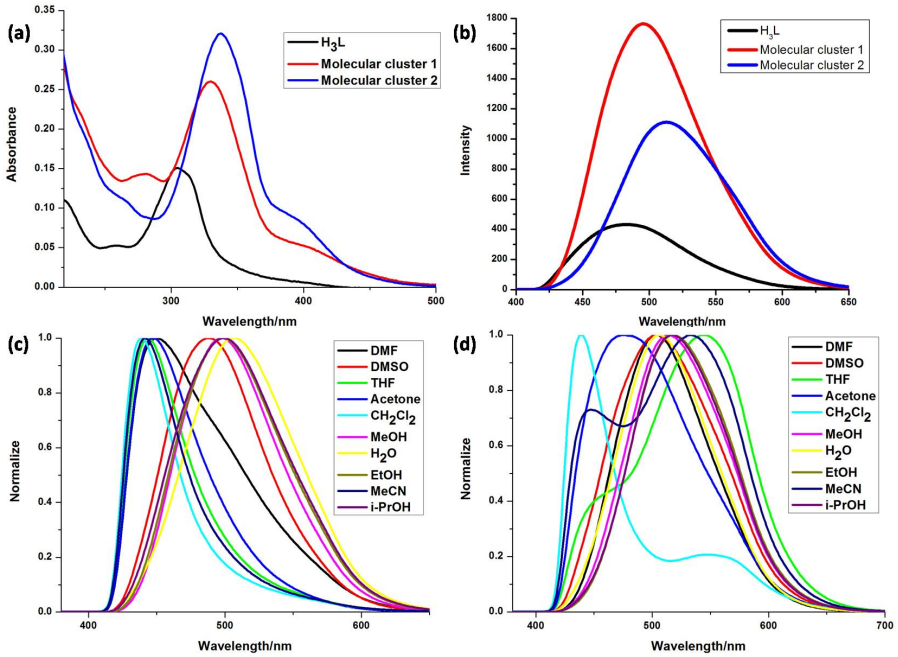

Fig. S14 (a) UV-vis spectra of the ligand **H_3L**, **1** and **2** in EtOH. (b) Fluorescence emission spectra of ligand **H_3L**, **1** and **2** in EtOH (10μM in ethanol solutions, λ_{ex}= 330 nm). Fluorescence spectra of the **1**(c) and **2**(d) in various solvents of different polarities, λ_{ex}= 330 nm.

References

1. (a) X. H. Peng, X. L. Tang, W. W. Qin, W. Dou, Y. L. Guo, J. R. Zheng, W. S. Liu, D. Q. Wang, *Dalton Trans.*,2011, **40**, 5271–5277.(b) L. N. Wang, W. W. Qin, X. L. Tang, W. Dou, W. S. Liu, *J. Phys. Chem. A,* 2011, **115**, 1609–1616. (c) Y. H. Lu, Y. W. Lu, C. L. Wu, Q. Shao, X. L. Chen, R. N. B. Bimbonga, *Spectrochim. Acta A,* 2006, **65**, 695–701.

2. (a) V. Chandrasekhar, R. Azhakar, B. Murugesapandian, T. Senapati, P. Bag, M. D. Pandey, S. K. Maurya, D. Goswami, *Inorg. Chem.* , 2010, ***49***, 4008–4016. (b) J. J. Lu, L. Zhang, L. Liu, G. F. Liu, D. Z. Jia, D. L. Wu, G. C . Xu, *Spectrochim. Acta A,* 2008, **71**, 1036–1041.